Study on the productivity of silicon nanoparticles by picosecond laser ablation in water: towards gram per hour yield

Romuald Intartaglia[1], **Komal Bagga**[1], **and Fernando Brandi**[1,2,*]

[1]*Istituto Italiano di Tecnologia, Nanophysics Department, via Morego 30, 16163 Genova, Italy*

[2]*Istituto Nazionale di Ottica, CNR, Via G. Moruzzi 1, 56124 Pisa, Italy*

[*] *fernando.brandi@iit.it, fernando.brandi@ino.it*

Abstract: An investigation on the productivity of silicon nanoparticles by picosecond laser ablation in water is presented. A systematic experimental study is performed as function of the laser wavelength, fluence and ablation time. In case of ablation at 1064 nm silicon nanoparticles with a mean diameter of 40 nm are produced. Instead, ablation at 355 nm results in nanoparticles with a mean diameter of 9 nm for short ablation time while the mean diameter decreases to 3 nm at longer ablation time. An original model based on the *in-situ* ablation/photo-fragmentation physical process is developed, and it very well explains the experimental productivity findings. The reported phenomenological model has a general validity, and it can be applied to analyze pulsed laser ablation in liquid in order to optimize the process parameters for higher productivity. Finally, an outlook is given towards gram per hour yield of ultra-small silicon nanoparticles.

OCIS codes: 350.3390 Laser materials processing, 220.4241 Nanostructure fabrication, 160.4236 Nanomaterials

References and links

1. R. Walters, G. Bourianoff, and H. Atwater, "Field-effect electroluminescence in silicon nanocrystals," Nat. Mater. **4,** 143-146 (2005).
2. G. Belomoin, J. Therrien, A. Smith, S. Rao, R. Twesten, S. Chaieb, M. H. Nayfeh, L. Wagner, and L. Mitas, "Observation of a magic discrete family of ultrabright Si nanoparticles," Appl. Phys. Lett. **80,** 841-843 (2002).
3. M. Stupca, M. Alsalhi, T. Al Saud, A. Almuhanna, and M. H. Nayfeh,"Enhancement of polychrystalline silicon solar cells using ultra thin films of silicon nanoparticle," Appl. Phys. Lett. **91,** 063107 (2007).
4. S. Alkis, F. B. Oruç, B. Ortaç, A. C. Koşger, and A. K. Okyay, "A plasmonic enhanced photodetector based on silicon nanocrystals obtained through laser ablation," J. Opt. **14,** 125001 (2012).
5. F. Erogbogbo, K. T. Yong, I. Roy, R. Hu, W. C. Law, W. W. Zhao, H. Ding, F. Wu, R. Kumar, M. T. Swihart, and P. N. Prasad, "In vivo targeted cancer imaging, sentinel lymph node mapping and multi-channel imaging with biocompatible silicon nanocrystals," ACS Nano **5,** 413-423 (2011).
6. Z. F. Li and E. Ruckenstein, "Water-soluble Poly(acrylic acid) grafted luminescent silicon nanoparticles and their use as fluorescent biological staining labels," Nano Lett. **4** 1463-1467 (2004).
7. S Chinnathambi, S. Chen, S. Ganesan, and N Hanagata, "Silicon quantum dots for biological applications," Adv. Healthcare Mater. doi: 10.1002/adhm.201300157 (2013).
8. Y. Zhong, F. Peng, F. Bao, S. Wang, X. Ji, L. Yang , Y. Su, S.-T. Lee, and Y. He, "Large-scale aqueous synthesis of fluorescent and biocompatible silicon nanoparticles and their use as highly photostable biological probes," J. Am. Chem. Soc. **135,** 8350-8356 (2013).

#202753 - $15.00 USD Received 12 Dec 2013; revised 10 Jan 2014; accepted 12 Jan 2014; published 3 Feb 2014

9. R. Intartaglia, K. Bagga, M. Scotto, A. Diaspro, and F. Brandi, "Luminescent silicon nanoparticles prepared by ultra short pulsed laser ablation in liquid for imaging applications," Opt. Mat. Express **2,** 510-518 (2012).
10. E. Borsella, M. Falconieri, N. Herlin, V. Loschenov, G. Miserocchi, Y. Nie, I. Rivolta, A. Ryabova, and D. Wang, "Biomedical and sensor applications of silicon nanoparticles," Silicon Nanocrystals: Fundamentals, Synthesis and Applications, ed. L. Pavesi and R. Turan, Wiley-VCH Verlag GmbH & Co. KGaA, Weinheim, Germany (2010).
11. L. Xiao, L. Gu, S. B. Howell, and M. J. Sailor, "Porous silicon nanoparticle photosensitizers for singlet oxygen and their phototoxicity against cancer cells," ACS Nano **5,** 3651-3659 (2011).
12. D. Rioux, M. Laferrière, A. Douplik, D. Shah, L. Lilge, A. V. Kabashin, and M. M. Meunier, "Silicon nanoparticles produced by femtosecond laser ablation in water as novel contamination-free photosensitizers," J. Biomed. Opt. **14,** 021010 (2009).
13. M. Rosso-Vasic, E. Spruijt, Z. Popovic, K. Overgaag, B. Van Lagen, B. Grandidier, D. Vanmaekelbergh, D. Dominguez-Gutierrez, L. De Cola, and H. Zuilhof, "Amine-terminated silicon nanoparticles: synthesis, optical properties and their use in bioimaging," J. Mater. Chem. **19,** 5926-5933 (2009).
14. L. Mangolini, "Synthesis, properties, and applications of silicon nanocrystals," J. Vac. Sci. Technol. B **31,** 020801 (2013).
15. D. Tan, S. Zhou, J. Qiu, and N. Khusroa, "Preparation of functional nanomaterials with femtosecond laser ablation in solution," J. Photochem. Photobiol. C-Photochem. Rev.**17,** 50-68 (2013).
16. H. Zeng, X.-W. Du, S. C. Singh, S. A. Kulinich, S. Yang, J. He, and W. Cai, "Nanomaterials via laser ablation/irradiation in liquid: a Review," Adv. Funct. Mater. **22,** 1333-1353 (2012).
17. V. Amendola and M. Meneghetti, "What controls the composition and the structure of nanomaterials generated by laser ablation in liquid solution?," Phys. Chem. Chem. Phys. **15,** 3027-3046 (2013).
18. H. Muto, K. Yamada, K. Miyajima, and F. Mafuné, "Estimation of surface oxide on surfactant-free gold nanoparticles laser-ablated in water," J. Phys. Chem. C **111,** 17221-17226 (2007).
19. S. Barcikowski and G. Compagnini, "Advanced nanoparticle generation and excitation by lasers in liquids," Phys. Chem. Chem. Phys. **15,** 3022-3026 (2013).
20. S. W. Mhin, J. H. Ryu, K. M. Kim, G. S. Park, H. W. Ryu, K. B. Shim, T. Sasaki, and N. Koshizaki, "Simple synthetic route for hydroxyapatite colloidal nanoparticles via a Nd:YAG laser ablation in liquid medium," Appl. Phys. A Mater. Sci. Process. **96,** 435-440 (2009).
21. Some companies producing and commercializing PLAL generated nanoparticles: PlasmaTech (Italy), http://www.plasmatech.it; Particular (Germany), http://www.particular.eu; I-Colloid (US), http://nano.imra.com; AlphaNov (France), http://www.alphanov.com.
22. R. Intartaglia, A. Barchanski, K. Bagga, A. Genovese, G. Das, P. Wagener, E. Di Fabrizio, A. Diaspro, F. Brandi, and S. Barcikowski "Bioconjugated silicon quantum dots from one-step green synthesis," Nanoscale **4,** 1271-1274 (2012).
23. K. Bagga, A. Barchanski, R. Intartaglia, S. Dante, R. Marotta, A. Diaspro, C. L. Sajti, and F. Brandi "Laser-assisted synthesis of *Staphylococcus aureus* protein-capped silicon quantum dots as bio-functional nanoprobes," Laser Phys. Lett. **10,** 065603 (2013).
24. K. Abderrafi, R. G. Calzada, M. B. Gongalsky, I. Suarez, R. Abarques, V. S. Chirvony, V. Y. Timoshenko, R. Ibanez, and J. P. Martinez-Pastor, "Silicon nanocrystals produced by nanosecond laser ablation in an organic liquid," J. Phys. Chem. C **115,** 5147-5151 (2011).
25. V. Švrček, D.Mariotti, and M.Kondo, "Ambient-stable blue luminescent silicon nanocrystals prepared by nanosecond-pulsed laser ablation in water," Opt. Express **17,** 520-527 (2009).
26. D. M. Popovic, J. S. Chai, A. A. Zekic, M. Trtica, M. Momcilovic, and S. Maletic, "Synthesis of silicon-based nanoparticles by 10.6 μm nanosecond CO_2 laser ablation in liquid," Laser Phys. Lett. **10,** 026001 (2013).
27. P. Chewchinda, T. Tsuge, H. Funakubo, O. Odawara , and H. Wada, "Laser wavelength effect on size and morphology of silicon nanoparticles prepared by laser ablation in liquid," J. J. Appl. Phys. **52,** 025001 (2013).
28. S. Yang, W. Cai, H. Zhang, X. Xu, and H. Zeng, "Size and structure of Si nanoparticles by laser ablation in different liquid media and further centrifugation classification," J. Phys. Chem. C **113,** 19091-19095 (2009).
29. K. Abderrafi, R. García-Calzada, J. F. Sanchez-Royo, V. S. Chirvony, Sa"ıd Agouram, R. Abargues, R. Ibáñez, and J. P. Martínez-Pastor, "Laser ablation of a silicon target in chloroform: formation of multilayer graphite nanostructures," J. Phys. D: Appl. Phys. **46,** 135301 (2013).
30. S. Alkis, A. K. Okyay, and B. Ortaç, "Post-Trearment of silicon nanocrystals produced by ultra-short pulsed laser ablation in liquid: towards blue luminescent nanocrystal generation," J. Phys. Chem.C **116,** 3432-3436 (2012).
31. P. G. Kuzmin, G. A. Shafeev, V. V. Bukin, S. V. Garnov, C. Farcau, R. Carles, B. Warot-Fontrose, V. Guieu, and G. Viau, "Silicon nanoparticles produced by femtosecond laser ablation in ethanol: size control, structural characterization, and optical properties," J. Phys. Chem. C **114,** 15266-15273 (2010).
32. R. Intartaglia, K. Bagga K, F. Brandi, G. Das, A. Genovese, E. Di Fabrizio, and A. Diaspro, "Optical properties of femtosecond laser-synthesized silicon nanoparticles in deionized water," J. Phys. Chem. C **115,** 5102-5107 (2011).
33. M. Tiberi, A. Simonelli, G. Cristoforetti, P. Marsili, F. Giammanco, and E. Giorgetti, " Effect of picosecond laser induced cavitation bubbles generated on Au targets in a nanoparticle production set-up," Appl. Phys. A **110,**

#202753 - $15.00 USD Received 12 Dec 2013; revised 10 Jan 2014; accepted 12 Jan 2014; published 3 Feb 2014

857-861 (2013).
34. N. Bärsch, J. Jakobi, S. Weiler, and S. Barcikowski, "Pure colloidal metal and ceramic nanoparticles from high-power picosecond laser ablation in water and acetone," Nanotechnology **20,** 445603 (2009).
35. P. A. Perminov, I. O. Dzhun, A. A. Ezhov, S. V. Zabotnov, L. A. Golovan, G. D. Ivlev, E. I. Gatskevich, V. L. Malevich, and P. K. Kashkarov, "Creation of silicon nanocrystals using the laser ablation in liquid," Laser Phys. **21,** 801-804 (2011).
36. O. I. Eroshova, P. A. Perminov, S. V. Zabotnov, M. B. Gongalskii, A. A. Ezhov, L. A. Golovan, and P. K. Kashkarov,"Structural properties of silicon nanoparticles formed by pulsed laser ablation in liquid media," Crystallogr. Rep., **57,** 831-835 (2012).
37. R. Intartaglia, K. Bagga, A. Genovese, A. Athanassiou, R. Cingolani, A. Diaspro, and F. Brandi, "Influence of organic solvent on optical and structural properties of ultra-small silicon dots synthesized by UV laser ablation in liquid," Phys. Chem. Chem. Phys. **14,** 15406-15411 (2012).
38. F. Giammanco, E. Giorgetti, P. Marsili, and A. Giusti, "Experimental and theoretical analysis of photofragmentation of Au nanoparticles by picosecond laser radiation," J. Phys. Chem. C **114,** 3354-3363 (2010).
39. D. Werner and S. Hashimoto, "Improved working model for interpreting the excitation wavelength and fluence-dependent response in pulsed laser-induced size reduction of aqueous gold nanoparticles," J. Phys. Chem. C **115,** 5063-5072 (2011).
40. A. Pyatenko, M. Yamaguchi, and M. Suzuki, "Mechanisms of size reduction of colloidal silver and gold nanoparticles irradiated by Nd:YAG laser," J. Phys. Chem. C **113,** 9078-9085 (2009).
41. F. Mafuné, J. Y. Kohno, Y. Takeda, and T. Kondow, "Dissociation and aggregation of gold nanoparticles under laser irradiation," J. Phys. Chem. B **105,** 9050-9056 (2001).
42. V. Švrček, D. Mariotti, T. Nagai, Y. Shibata, I. Turkevych, and M. Kondo, "Photovoltaic applications of silicon nanocrystal based nanostructures induced by nanosecond laser fragmentation in liquid media," J. Phys. Chem. C **115,** 5084-5093 (2011).
43. R. Intartaglia, G. Das, K. Bagga, A. Gopalakrishanan, A. Genovese, M. Povia, E. Di Fabrizio, R. Cingolani, A. Diaspro, and F. Brandi, "Laser synthesis of ligand-free bimetallic nanoparticles for plasmonic applications," Phys. Chem. Chem. Phys. **15,** 3075-3082 (2013).
44. H. Wang, A. Pyatenko, K. Kawaguchi, X. Li, Z. Swiatkowska-Warkocka, and N. Koshizaki, "Selective pulsed heating for the synthesis of semiconductor and metal submicrometer spheres," Angew. Chem. Int. Ed. **49,** 6361 6364 (2010).
45. Z. Swiatkowska-Warkocka, K. Koga, K. Kawaguchi, H. Wang, A. Pyatenko, and N. Koshizaki, "Pulsed laser irradiation of colloidal nanoparticles: a new synthesis route for the production of non-equilibrium bimetallic alloy submicrometer spheres," RSC Adv. **3,** 79-83 (2013).
46. A. Pyatenko, H. Wang, N. Koshizaki, and T. Tsuji, "Mechanism of pulse laser interaction with colloidal nanoparticles," Laser & Photon. Rev. **7,** 596604 (2013).
47. V. Švrček, T. Sasaki, Y.Shimizu, and N. Koshizaki, "Silicon nanocrystals formed by pulsed laser-induced fragmentation of electrochemically etched Si micrograins," Chem. Phys. Lett. **429,** 483487 (2006).
48. A. Schwenke, P. Wagener, S. Nolte, and S. Barcikowski, "Influence of processing time on nanoparticle generation during picosecond-pulsed fundamental and second harmonic laser ablation of metals in tetrahydrofuran," Appl. Phys. A **104,** 77-82 (2011).
49. H. Muto, K. Miyajima, and F. Mafuné, "Mechanism of laser-induced size reduction of gold nanoparticles as studied by single and double laser pulse excitation," J. Phys. Chem. C **112,** 5810-5815 (2008).
50. F. Mafuné, J. Y. Kohno, Y. Takeda, and T. Kondow, "Formation of gold nanoparticles by laser ablation in aqueous solution of surfactant," J. Phys. Chem. B **105,** 5114-5120 (2001).
51. O. Van Overschelde, J. Dervaux, L. Yonge, D. Thiry, and R. Snyders, "Screening effect in gold nanoparticles generated in liquid by KrF ablation," Laser Phys. **23,** 055901 (2013).
52. P. Blandin, K. A. Maximova, M. B. Gonglasky, J. F. Sanchez-Royo, V. S. Chirvony, M. Sentis, V. Y. Timoshenko, and A. V. Kabashin, "Femtosecond laser fragmentation from water-dispersed microcolloids: toward fast controllable growth of ultrapure Si-based nanomaterials for biological applications," J. Mater. Chem. B **1,** 2489-2495 (2013).
53. F. Brandi, N. Burdet, R. Carzino, and A. Diaspro, "Very large spot size effect in nanosecond laser drilling efficiency of silicon," Opt. Express **18,** 23488-23494 (2010).
54. C. L. Sajti, R. Sattari, B. N. Chichkov, and S. Barcikowski, "Gram scale synthesis of pure ceramic nanoparticles by laser ablation in liquid," J. Phys. Chem. C **114,** 2421-2427 (2010).
55. P. Wagener, A. Schwenke, B. N. Chichkov, and S. Barcikowski, "Pulsed laser ablation of zinc in Tetrahydrofuran: bypassing the cavitation bubble," J. Phys. Chem. C **114,** 7618-7625 (2010).
56. S. Alkis, M. Alevli, S. Burzhuev, H. A. Vural, A. K. Okyay, and B. Ortaç, "Generation of InN nanocrystals in organic solution through laser ablation of high pressure chemical vapor deposition grown InN thin film," J. Nanopart. Res. **14,** 1048 (2012).
57. J. Jiang, P. Liu, Y. Liang, H. B. Li, and G. W. Yang, "Promoting the yield of nanoparticles from laser ablation in liquid," Appl. Phys. A **105,** 903-907 (2011).
58. T. Salminen, J. Dahl, M. Tuominen, P. Laukkanen, E. Arola, and T. Niemi, "Single-step fabrication of lumines-

#202753 - $15.00 USD Received 12 Dec 2013; revised 10 Jan 2014; accepted 12 Jan 2014; published 3 Feb 2014

cent GaAs nanocrystals by pulsed laser ablation in liquids," Opt. Mat. Express **2,** 799-813 (2012).
59. K. Abderrafi, E. Jiménez, T. Ben, S. I. Molina, R. Ibáñez, V. Chirvony, J. P. Martínez-Pastor, "Production of Nanometer-Size GaAs Nanocristals by Nanosecond Laser Ablation in Liquid," J. Nanosci. Nanotechnol. **12,** 6774-6778 (2012).

1. Introduction

Ultra-small luminescent silicon nanoparticles (Si-NPs) with diameters in the range 1-3 nm are very good candidates for various applications ranging from light-emitting devices [1, 2], to photo-voltaic solar cell technology and optoelectronics [3, 4]. Biocompatibility and stability against photo-bleaching make of these nanoparticles ideal substitute to dyes as fluorescent labels for imaging [5–10], as well as efficient photosesitizer for treatments [11, 12].

Many methods have been developed for the synthesis of Si-NPs, such as solution chemistry routes [8, 11, 13], thermal decomposition and laser pyrolysis of silane, laser ablation of solid target in vacuum or controlled atmosphere, and nonthermal plasma synthesis [14].

An alternative method for the production of stable nanoparticle colloidal solutions is Pulsed Laser Ablation in Liquid (PLAL) which has significantly emerged in the past years [15–20]. PLAL is nowadays a well established approach for the synthesis and commercialization of nanoparticle colloidal solutions [21]. PLAL has several advantages compared with other methods: i) it is a clean synthesis, without the need of chemical precursors and reducing agents, resulting in highly-pure and stable nanoparticles; ii) it is simple and economical, since it is performed at ambient conditions; iii) it is versatile, since the obtained NPs are in colloidal solution form, giving the opportunity of further nanoscale manipulations, such as biofunctionalization [22, 23].

The synthesis of Si-NPs by PLAL in various solvents has been extensively investigated using laser with ns [24–29] and fs [9, 12, 30–32] pulse duration.
PLAL of silicon with $\sim$ 10 ns and longer laser pulses involves substantial melting of the substrate as well as interaction of the laser pulse with the generated cavitation bubble, often leading to the production of large NPs, a silicon oxide matrix, and NP clusters, while preventing the synthesis of ultra-small Si-NPs in water. Therefore, ablation with shorter laser pulses is preferable for the production of ultra-small Si-NP colloidal solutions by PLAL since both the thermal effects and the interaction of the laser pulse with the cavitation bubble are minimized [33].
In the perspective to achieve high production yield of NPs by PLAL, the use of ps laser is potentially more attractive compared with the use of fs laser given the recent advances in ps laser technology towards high average power. Indeed, a high PLAL productivity of metallic and ceramic NPs has been reported using high-power ps laser [34].
To our knowledge, there have been few studies on PLAL of silicon using ps laser. It is reported that PLAL of silicon in water using 30 ps NIR laser pulses leads to the generation of Si-NPs with a broad size distribution peaked around 20 nm [35, 36]. Recently, we reported on the production and characterization of ultra-small photoluminescent Si-NPs with a diameter of 3 nm by ultra-violet (UV) ps PLAL in water and toluene [37].

In order to optimize the production yield of ultra-small Si-NPs by ps PLAL it is necessary to better understand the physical mechanism behind such process. A well known mechanism to reduce the size of NPs in a colloidal solution is photo-fragmentation, i.e., the fragmentation of large NPs into small NPs by pulsed laser irradiation of the colloidal solution. NPs photo-fragmentation is strongly related to the optical absorption properties of the colloidal solution, and it has been investigated either *ex-situ* [38–47], i.e., by irradiation of the NPs colloidal solution, or *in-situ* [48–51], i.e., during NPs generation by PLAL. Recently, photo-fragmentation of silicon micro-colloids with a fs NIR laser has been reported resulting in the production of stable photoluminescent Si-NP colloidal solution [52].

#202753 - $15.00 USD Received 12 Dec 2013; revised 10 Jan 2014; accepted 12 Jan 2014; published 3 Feb 2014

In the present article a systematic study on the productivity of Si-NPs by ps PLAL of bulk silicon in water as function of laser fluence and wavelength is reported. It is found that the phenomenon leading to the production of ultra-small Si-NPs by ps UV PLAL is *in-situ* photo-fragmentation. Instead, ps NIR PLAL of silicon in water does not involve photo-fragmentation, which leads to the production of larger Si-NPs. A physical model based on a phenomenological interpretation of the *in-situ* ablation/photo-fragmentation process is developed, resulting in an analytical equation that very well explains the experimental findings. The model has a general validity, and therefore can be applied to analyze PLAL experiment results in order to optimize the process parameters, i.e., laser wavelength, pulse duration, and fluence, towards higher productivity.

2. Experimental details

2.1. Pulsed laser ablation of silicon in water

PLAL of silicon in water is performed using the NIR fundamental beam at 1064 nm, and the UV third-harmonic beam at 355 nm, of a mode-locked amplified Nd:YAG laser (Leopard, Continuum) providing pulses of 60 ps time duration, at a repetition rate of 20 Hz. The laser beam profile is flat-top thanks to a serrated aperture relay imaging between the oscillator and the amplifier. The silicon target (99.999% from Alpha Aesar), in the form of cylinder with diameter of 6 mm and thickness of 10 mm, is placed on the bottom of a quartz cuvette (dimension 10x10x30 mm^3) and immersed in 2 ml of deionized water, resulting in about 13 mm of water above the silicon target surface. The laser beam is focused below the silicon target surface using a lens with a focal length of 30 cm. The target position is adjusted in both UV and NIR PLAL experiments in order to have a UV and NIR beam spot diameter on the target of 0.2 mm. PLAL experiments are performed as function of ablation time and for various laser pulse fluence, controlled by means of suitable variable attenuators. Before each experiment the target is mechanically polished and then washed several times with water in order to remove impurity from the surface. During laser ablation, the target is moved with a motorized stage system to achieve uniform ablation of the silicon surface.

2.2. Characterization

The quantity of silicon in the obtained colloidal solutions is evaluated by Inductively Coupled Plasma Optical Emission Spectrometry (ICAP 6300, Duo Thermo Scientific). For this measurements, 100 μl solution of Si-NPs is introduced in Aqua regia, and after overnight acid digestion the final volume is adjusted with Milli-Q water to 25 ml. The dilution factor is kept into consideration while determination of final concentration.
Transmission electron microscopy (TEM) imaging is performed working at an acceleration voltage of 100 kV (JEOL 1011 microscope). For sample preparation, a drop of the Si-NPs colloidal solutions is deposited and dried directly onto carbon-coated 300 mesh copper grid.
A 100 μl colloidal solution is used to measure the absorption spectra using a spectrophotometer (Cary 6000). Photoluminescent (PL) measurements are carried out with a spectrofluorometer (Fluoroma-4, Jobin Yvon-Horiba) exciting at 290 nm .

3. Results and discussion

3.1. Productivity and size of Si-NPs

Figure 1 shows the experimental results concerning the ablated silicon mass in the colloidal solution as function of number of laser pulses, i.e., ablation time, for various laser pulse fluence,

#202753 - $15.00 USD Received 12 Dec 2013; revised 10 Jan 2014; accepted 12 Jan 2014; published 3 Feb 2014

along with the TEM images of the produced Si-NPs.

In case of NIR PLAL a clear linear increase of the ablated mass as function of ablation time is found for fluence in the range 0.9 to 2.7 J cm^{-2}, as shown in Fig. 1(a). UV-vis absorption spectroscopy measurement of the colloidal solution obtained after 60 min of ablation (72000 laser pulses) at 2.7 J cm^{-2} is reported in the inset of Fig. 1(a). The absorption spectrum has a broad band between 200 and 800 nm with a shoulder around 500 nm, which is characteristic of Si-NPs population with mean diameter of tens of nm [32]. Complementary electron microscopy study of the Si-NPs obtained after 60 min of NIR PLAL at a fluence of 2.7 J cm^{-2} confirms a mean diameter of about 40 nm, as shown by the TEM image in Fig. 1(c).

Instead, in case of UV PLAL with fluence in the range 0.4 to 4.4 J cm^{-2} two very distinct time regimes are observed. As shown in Fig. 1(b), an initial phase (*transient regime*) is followed by a second phase (*steady state regime*) with a lower and clearly constant ablation rate. Indeed, the Si-NPs produced in the two UV PLAL regimes have different size: Si-NPs with mean diameter of about 9 nm are produced in the *transient regime*, as shown by the TEM image in Fig. 1(d), while ultra-small Si-NPs with mean diameter of 3 nm are produced in the *steady state regime*, as shown by the TEM image in Fig. 1(e). The production of ultra-small Si-NPs after 60 min of UV PLAL is confirmed also by UV-Vis absorption spectroscopy reported in the inset of Fig. 1(a), where the absorption spectrum of the colloidal solution obtained with UV PLAL at a fluence of 3 J cm^{-2} is shown: a significant increase in the UV absorption (below 300 nm) typical of ultra-small Si-NPs [32] is observed. It is noted that larger Si-NPs are very rarely produced by UV PLAL. The inset in Fig. 1(b) shows the PL spectrum of the Si-NPs produced by UV PLAL after 72000 laser pulses at a fluence of 3 J cm^{-2}. The optical properties of the obtained Si-NPs, i.e., UV-vis absorption and PL spectra, remain the same for several months indicating a high stability of the colloidal solutions, which is of great importance for practical applications.

The linear increase of the ablated mass in case of NIR PLAL indicates no interaction between NIR laser pulses and the Si-NPs colloidal solution, while the presence of the two very distinct UV PLAL regimes suggests a strong time dependent interaction between the UV laser beam and the Si-NPs colloidal solution.

3.2. *PLAL efficiency model*

In order to elucidate the mechanism leading to the production of ultra-small Si-NPs, the ablation efficiency, i.e., ablated mass per single laser pulse, in the different experimental conditions is analyzed. The ablation efficiencies are given by the slope of the straight lines resulting from the least-square linear fits on the experimental data reported in Fig. 1. It is noted that in the *transient regime* of UV PLAL the linear fit on the experimental data gives a first order approximation of the actual ablation rate. This is evident from the fact that the straight lines resulting from the fit do not pass through the origin, i.e., zero ablated mass at zero ablation time.

To analyze the ablation efficiency data a phenomenological model based on ablation and *in-situ* photo-fragmentation is developed as follows.

i) Ablation The ablation depth, i.e., the thickness of the ablated layer per single laser pulse, is given by,

$$T = K \times \ln(F_t/F_{th}), \tag{1}$$

where F_t is the laser fluence on the target, F_{th} is the fluence threshold for ablation, and K is a phenomenological parameter [53]. Typically, K is related both to the absorption depth of the light in the bulk material (for silicon about 10 nm at 355 nm and few hundreds micron at 1064 nm, at room temperature), and to the thermal diffusion length $2\sqrt{D \times \tau}$, where D is the thermal diffusivity and τ is the laser pulse duration. For $\tau \sim 60$ ps the thermal diffusion length in silicon

#202753 - $15.00 USD Received 12 Dec 2013; revised 10 Jan 2014; accepted 12 Jan 2014; published 3 Feb 2014

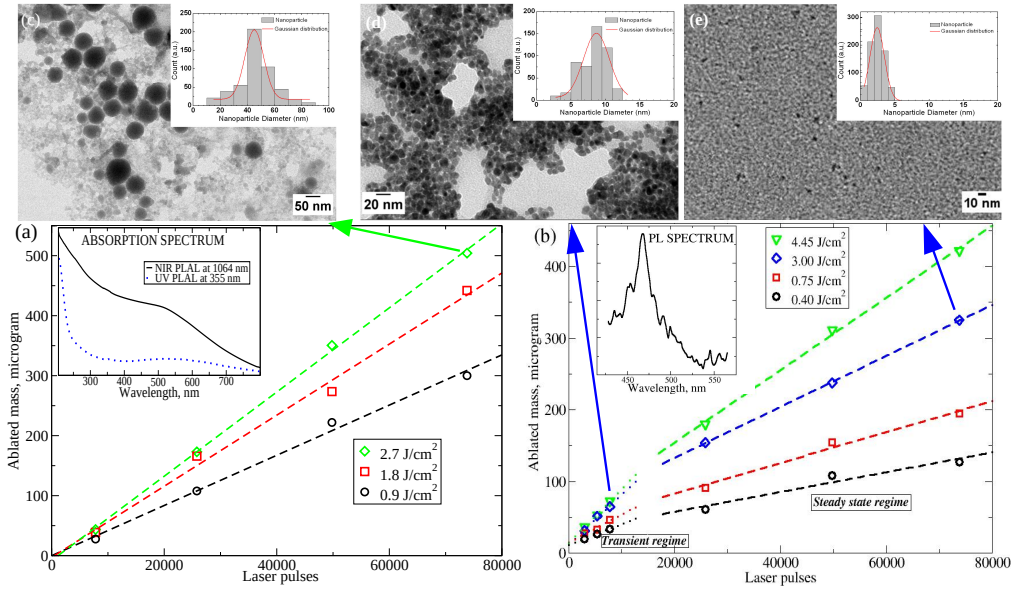

Fig. 1. Ablated silicon mass as function of the number of laser pulses (ablation time), and TEM images with size distribution of the produced Si-NPs. Graph (a) and (b) show the ablated silicon mass as function of number of laser pulses for NIR and UV PLAL respectively. The straight lines over the experimental data points result from the least-square linear fits. The insets in graph (a) and (b) show the measured absorption and photoluminescent spectra of the produced Si-NPs respectively. TEM images and size distribution of Si-NPs produced by PLAL in water: (c), NIR PLAL at 2.7 J cm^{-2} after 72000 laser pulses; (d), UV PLAL at 3 J cm^{-2} after 6000 laser pulses, i.e., 5 min ablation time; (e), UV PLAL at 3 J cm^{-2} after 72000 laser pulses.

is about 140 nm (D_{Si}=0.85 cm^2 s^{-1} at room temperature). Using Eq. (1), the ablation efficiency is given by,

$$M_a \equiv \rho \times S \times T = \rho \times S \times K \times \ln(F_t/F_{th}), \tag{2}$$

where ρ is the bulk density (2.3 g cm^{-3} for silicon) and $S = 3 \times 10^{-4}$ cm^2 is the laser spot area on the target surface.

ii) Photo-fragmentation The laser pulse energy may be actually reduced during propagation in the colloidal solution due to the interaction with the NPs, eventually leading to photo-fragmentation. During the experiments the energy of the laser pulses E_0 is measured before the laser beam propagates into the liquid, so $F_0 = E_0 \times S^{-1}$ is the fluence on the target as if there was no energy loss during propagation in the colloidal solution. Therefore, an *apparent* ablation threshold is defined as $F_{th}^{app} = F_{th} \times F_0 \times (F_t)^{-1}$ taking into account the laser energy loss in the colloidal solution. Substituting $F_t \times (F_{th})^{-1}$ with $F_0 \times (F_{th}^{app})^{-1}$ in Eq. (2) the PLAL efficiency including photo-fragmentation effect is given by,

$$M_a = \rho \times S \times K \times \ln(F_0/F_{th}^{app}). \tag{3}$$

Note that, without laser energy loss in the colloidal solution $F_t = F_0$, and thus $F_{th} = F_{th}^{app}$.

#202753 - $15.00 USD Received 12 Dec 2013; revised 10 Jan 2014; accepted 12 Jan 2014; published 3 Feb 2014

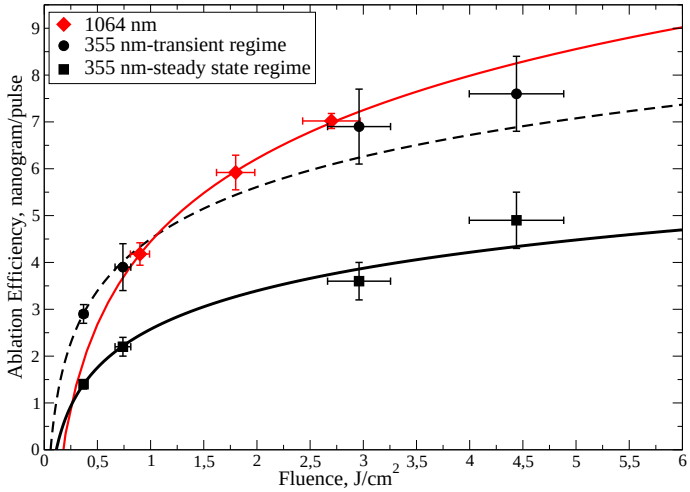

Fig. 2. Silicon ablation efficiency of ps PLAL in water; the error bars result from the least-square fit performed on the experimental data points in Fig. 1, and from the uncertainty on the measured laser pulse energy; the curves are the result of a logarithmic fit as from the ablation efficiency model, see Eq. (3).

Table 1. Data analysis results for the silicon ablation efficiency of ps PLAL in water. The parameters K and F_{th}^{app}, along with the reported uncertainty, result from the logarithmic fit shown in Fig. 2. The Si-NPs mean size is found from TEM imaging analysis reported in Fig. 1, and the value in parenthesis is the size standard deviation. In the last column, the efficiency parameter described in Section 4 is reported.

Wavelength-data set	K, nm	F_{th}^{app}, J cm^{-2}	Si-NPs size, nm	η, 10^{-5}g J^{-1}
1064 nm	36(6)	0.18(1)	40(10)	1.7
355 nm-*transient regime*	22(4)	0.07(2)	9(2)	2.7
355 nm-*steady state regime*	17(2)	0.11(1)	3(1)	1.3

3.3. *Data analysis*

The ablation efficiency as function of laser fluence, found from the linear fit in Fig. 1, is reported in Fig. 2 for the different data set, along with the logarithmic fit of the data points, as from Eq. (3). The parameters K and F_{th}^{app} resulting from the logarithmic fitting curves are reported in Table 1, along with the Si-NPs size as found from TEM image analysis reported in Fig. 1.
The ablation depth parameter K for UV PLAL is found to be the same, within the error margins, in both *transient* and *steady state* regimes, with a mean value around 20 nm. This finding supports our model since for UV ps pulses the ablation depth value in silicon is in between the optical absorption depth (10 nm) and the thermal diffusion length (140 nm) [53]. On the other hand, the smaller *apparent* ablation threshold fluence for UV PLAL in the *transient regime*, 0.07 J cm^{-2}, compared to that in the *steady state regime*, 0.11 J cm^{-2}, is a consequence of the lower laser energy reaching the target surface in the *steady state regime* due to the energy loss during the propagation in the colloidal solution. It is noted that the higher uncertainty on the parameters K and F_{th}^{app} from the *transient regime* data set reflects the first order approximation

#202753 - $15.00 USD Received 12 Dec 2013; revised 10 Jan 2014; accepted 12 Jan 2014; published 3 Feb 2014

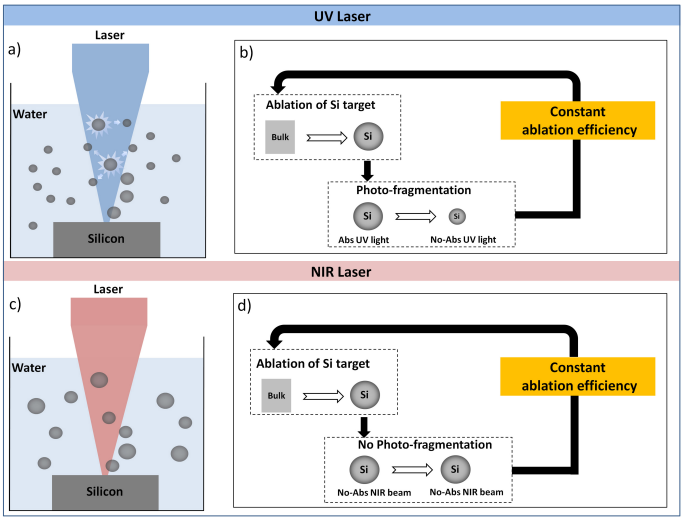

Fig. 3. Schematic of *in-situ* ablation/photo-fragmentation process during PLAL of silicon in water. UV PLAL: a) schematic of ablation and *in-situ* photo-fragmentation; b) ablation and *in-situ* photo-fragmentation process loop in the *steady state regime* leading to constant ablation efficiency. NIR PLAL: c) schematic of ablation without photo-fragmentation; d) ablation without photo-fragmentation process loop leading to constant ablation efficiency.

made in the linear fit shown in Fig. 1(b).
For NIR PLAL, K is about 36 nm while the *apparent* ablation threshold fluence is 0.18 J cm^{-2}. The higher ablation efficiency and apparent threshold for NIR PLAL compared with UV PLAL is consistent the larger optical absorption depth of NIR light in silicon bulk.

3.4. *In-situ ablation/photo-fragmentation of silicon nanoparticles*

The result of the data analysis and in particular the constant PLAL efficiency at longer ablation time, is explained by an *in-situ* ablation/photo-fragmentation process which is substantially different between UV and NIR ablation, as depicted in the schematic reported in Fig. 3.

In case of UV PLAL the ablation process leads first to the production of Si-NPs with diameter of about 9 nm, like in the *transient regime* (see Fig. 1(b)). Subsequently, these Si-NPs diffuse into the solvent, absorb the UV laser pulses, and are therefore photo-fragmented, producing ultra-small Si-NPs, as schematically shown in Fig. 3(a). Finally, the ultra-small Si-NPs having a much lower optical absorption at 355 nm (see inset in Fig. 1(a)), do not interact further with the UV laser pulse, resulting in a *steady state* loop, i.e., *steady state regime*, as shown in Fig. 3(b). It must be noted that for short ablation time in UV PLAL (i.e., in the *transient regime*) there is not a uniform distribution of NPs in the liquid medium confined in the cuvette, and the subsequent diffusion of NPs in the liquid lowers the actual NPs concentration along the laser beam path. Therefore, the incoming UV laser pulses are not absorbed efficiently by the ablated Si-NPs in the colloidal solution, resulting in a lower photo-fragmentation efficiency, i.e., a higher fluence on the target, and therefore higher ablation rate, as shown by the experimental findings and the data analysis. On the contrary, in the *steady state regime* the ablation/photo-fragmentation process reaches an equilibrium between the rate of Si-NPs produced by ablation and those photo-fragmented by the UV laser pulse, as schematically shown in Fig. 3(b). Photo-fragmentation reduces the laser energy reaching the bulk silicon target, and

#202753 - $15.00 USD Received 12 Dec 2013; revised 10 Jan 2014; accepted 12 Jan 2014; published 3 Feb 2014

therefore it is responsible for the lower ablation efficiency in the *steady state regime*.

Instead, during NIR PLAL there is not interaction between the laser pulse and the Si-NPs in the colloidal solution, as schematically shown in Fig. 3(c). Therefore, photo-fragmentation does not occur, resulting in a constant ablation efficiency regardless of the ablation time, as highlighted in Fig. 3(d).

In summary, the present analysis based on an phenomenological physical model indicates that the interplay between ablation and photo-fragmentation is at the origin of the production of ultra-small Si-NPs by UV PLAL.

4. Outlook: PLAL optimization towards gram per hour yield of ultra-small Si-NPs

With the parameters K and F_{th}^{app} found from PLAL experiments and data analysis, the developed model allows to evaluate the optimal parameters in order to maximize productivity of PLAL. In general, the given experimental parameter in PLAL is the energy per pulse E_0 available at a certain repetition rate RR from the laser source, while the optimal fluence, i.e., spot size on target, maximizing the yield has to be found. To do this, the Eq. (3) is rewritten as

$$M_a = \frac{\rho \times K \times E_0}{F_{th}^{app}} \times \frac{F_{th}^{app}}{F_0} \ln\left(\frac{F_0}{F_{th}^{app}}\right). \tag{4}$$

The function $y = x^{-1}\ln(x)$ has the maximum value of $y_{max} = e^{-1}$ at $x_{max} = e$, and therefore the maximum efficiency is

$$M_{a,max} = \frac{\rho \times K}{e \times F_{th}^{app}} \times E_0 = \eta \times E_0, \tag{5}$$

at $F_{0,max} = e \times F_{th}^{app}$ which corresponds to a spot area of $S_{max} = E_0 \times (e \times F_{th}^{app})^{-1}$. The values of the efficiency parameter $\eta = (\rho \times K) \times (e \times F_{th}^{app})^{-1}$ found in this study are reported in the last column of Table 1. Therefore, the maximum yield per second is $\eta \times E_0 \times RR = \eta \times P_{avg}$, where P_{avg} is the laser average power.

As outlook lets first consider the production of Si-NPs by ablation of bulk silicon in water with a 1064 nm picosecond laser having $P_{avg} = 100$ W (e.g., $E_0 = 1$ mJ and $RR = 100$ kHz). For 1 hour of ablation time, the estimated yield at maximum efficiency is around 6 g. Instead, using a 355 nm picosecond laser having $P_{avg} = 30$ W (e.g., $E_0 = 0.3$ mJ and $RR = 100$ kHz) the yield at maximum efficiency of ultra-small Si-NPs is estimated to be 1.4 g per hour. It is noted that the laser system performances considered for these estimates can be achieved through power amplification of mode-locked picosecond NIR laser using for example disk or slab amplifiers.
In this outlook, the effect due to pulse to pulse interaction through the cavitation bubble when high repetition rate lasers are used [54, 55], as well as eventual substantial absorption in the colloidal solution due to very high NPs density are neglected. The first of these effects can be controlled by proper motion of laser beam or target, while the second can be handled by implementing a liquid flow system.
In the perspective to achieve a high production yield of ultra-small Si-NPs, the use of multi-harmonic laser beam is foreseen applying the fundamental beam for production of NPs and the third-harmonic beam for photo-fragmentation (combined eventually with the second-harmonic beam for optimal usage of laser energy).

5. Conclusions

Picosecond PLAL of silicon in water is investigated aiming at the optimization of the production of ultra-small photoluminescent Si-NPs. It is found that UV PLAL leads to the production of Si-NPs with mean diameter of 3 nm, while NIR PLAL generates larger Si-NPs with mean diameter of about 40 nm. In order to explain these experimental findings a systematic study is

#202753 - $15.00 USD Received 12 Dec 2013; revised 10 Jan 2014; accepted 12 Jan 2014; published 3 Feb 2014

performed, and it is demonstrated that the interplay between ablation and photo-fragmentation of silicon by UV ps irradiation is at the origin of the production of ultra-small Si-NPs. A physical model based on *in-situ* ablation/photo-fragmentation process is developed and it very well explains the experimental findings. The presented physical model of PLAL, that combines the phenomenological description of laser ablation and photo-fragmentation, has a general validity, and therefore can be applied to analyze and optimize PLAL process also with other materials (e.g., semiconductors like InN [56], Ge [57], and GaAs [58, 59]).

Acknowledgments

The authors gratefully acknowledge Marco Scotto d'Abbusco for technical assistance, Simone Nitti for Inductively Coupled Plasma analysis, and the Istituto Italiano di Tecnologia for supporting this study.

#202753 - $15.00 USD Received 12 Dec 2013; revised 10 Jan 2014; accepted 12 Jan 2014; published 3 Feb 2014